Optical Materials 86 (2018) 239–246

Contents lists available at ScienceDirect

Optical Materials

journal homepage: www.elsevier.com/locate/optmat

Influence of nanostructured TiO_2 film thickness in dye-sensitized solar cells using naturally extracted dye from *Thunbergia erecta* flowers as a photosensitizer

B.C. Ferreira, D.M. Sampaio, R. Suresh Babu*, A.L.F. de Barros

Laboratory of Experimental and Applied Physics, Centro Federal de Educação Tecnológica, Celso Suckow da Fonseca (CEFET/RJ), Av. Maracanã Campus 229, Rio de Janeiro, 20271-110, Brazil

ARTICLE INFO

Keywords:
Dye-sensitized solar cells
Natural dyes
Photovoltaics
Nanostructured semiconductors
TiO_2 thin film
Photosensitizers

ABSTRACT

Dye-sensitized solar cells (DSSCs) have been considered as an alternative energy resource in recent years, due to low-cost fabrication and non-toxic compared to silicon-based and thin film solar cells. Herein, the natural dye containing anthocyanins were extracted from *Thunbergia erecta* natural flower petals by simple extraction techniques and used as photosensitizers in the DSSC. The extracts showed the UV–Vis absorptions in the 400–800 nm range with broad maxima in visible region around 537 nm. Fourier transform infrared (FTIR) spectrum was obtained after the dye coating on a semi-conductive layer, to identify the presence of anthocyanin according to the functional groups present in the dye molecules. To precise and progressive optimization of the TiO_2 photoanodes film thicknesses were prepared by spin coating technique and characterized by atomic force microscopy, field emission scanning electron microscopy and *J-V* characteristics. The photovoltaic performance studies were carried out to understand the effect of the TiO_2 multilayer photoanodes and the interaction with the dye molecules on the cells efficiency. Photovoltaic parameters like short circuit current (J_{SC}), open circuit voltage (V_{OC}) and fill factor (*FF*) were evaluated for fabricated cells. The optimized film thickness of the TiO_2 photoanode is ~5.5 μm with an efficiency of 0.37% under AM 1.5G illumination of sunlight. The V_{OC} of DSSCs gradually decreases as the thickness increases of the TiO_2 thin film and the highest conversion efficiency while it has the maximum short-circuit current density.

1. Introduction

Alternative renewable energy sources are the major concern of recent decades, owing to the great demand for the creation of equipment and devices that meet our increasing energy demand. The constant depletion of fossil fuels in the earth crust and the serious environmental problems accompanying their combustion, modern society has been searching for a new form of alternative energy that is a clean, renewable, cheap, safe and viable alternative to fossil fuels and nuclear energy [1]. However, renewable energy resources can be used, which cannot be exhausted and do not affect seriously in the environment. Solar energy is an interesting choice, for the photovoltaic cells are used to convert solar energy into electric energy [2]. From the array of solar cells, dye-sensitized solar cells (DSSCs) are the third generation of solar cells, developed by O'Regan and Gratzel in 1991 [3], which are considered as a promising alternative for silicon-based and thin film solar cells because of the low manufacturing cost, non-toxic and reasonably high conversion efficiency [4]. A schematic representation of DSSC is shown in Fig. 1a. It consists of three main components: a dye-sensitized semiconductor photo-anode, an electrolyte with a redox couple and a conductive counter electrode. One of the main points that favors to improve the efficiency of the DSSCs is the absorption spectrum of the photosensitizer dye, besides providing electrons for the conduction band of TiO_2, promoting an efficient electrons cycle [5]. The photosensitizer dye represents the core component of the DSSCs and has the function of photons' reception and anode sensitization, the working principle is representing in Fig. 1b. Generally, heavy transition metal complexes such as ruthenium polypyridyl based complexes are considered as good photosensitizers for DSSCs because of their extreme absorption over the entire visible range, highly stable excitation state (s), and very efficient metal-to-ligand charge transfer [6]. Conversion efficiency exceeding 11–12% could be obtained with the use of ruthenium-based photosensitizers [7]. However, the main disadvantage of ruthenium polypyridyl complex is high cost, environmental pollution

* Corresponding author.
E-mail address: suresh.rajendran@aluno.cefet-rj.br (R. Suresh Babu).

https://doi.org/10.1016/j.optmat.2018.10.016
Received 7 August 2018; Received in revised form 4 September 2018; Accepted 8 October 2018

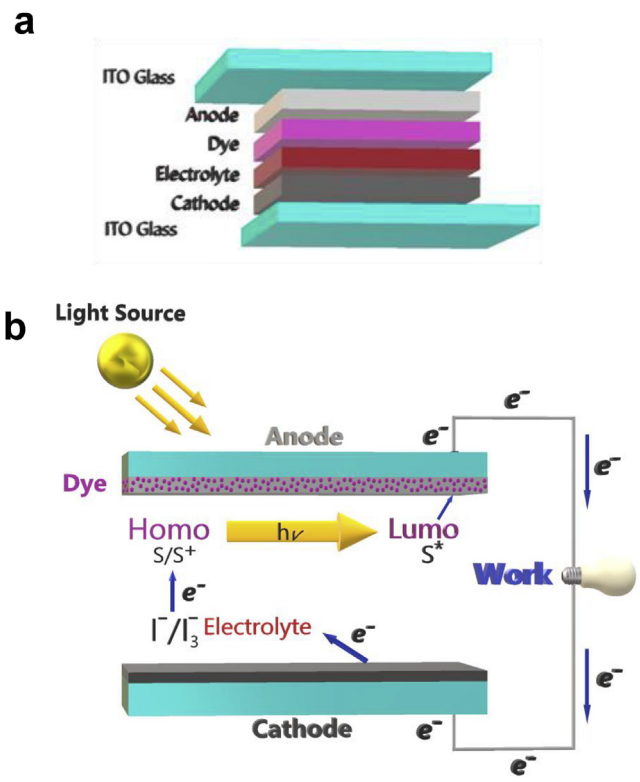

Fig. 1. Typical scheme (a) and working principle (b) of assembled DSSC.

and long-term unavailability of these noble metals [8,9], so need to search for alternative photosensitizers to be used for semiconductor-based photovoltaic devices [1,10]. Hence, many attempts have been made for the extraction of natural dyes and explore the possibility of their use as sensitizer dye in DSSCs.

Recently, natural dyes extracted from the various parts of the plants such as fruits, flowers leaves, and vegetables have been successfully used as photosensitizers in DSSC and have shown acceptable light-to-electricity conversion efficiency, low-cost, easy preparation, environment friendliness and large absorption coefficients. Several natural pigments containing anthocyanin, betalains, chlorophyll, tannin, and carotene have been successfully used as photosensitizers in the DSSCs [11–16]. The natural pigments were present in the various part of the plant including fruits, leaves, stems roots and flower petals. Amongst, anthocyanins belong to the group of natural dyes responsible for several colors and have a very large amount of red–blue plant pigments, which is naturally, occurs in all plants. Anthocyanins contain the functional group of carbonyl (-C═O) and hydroxyl (−OH) to bind the surface of the semiconductor TiO_2. This important parameter makes an efficient electron transfer from the anthocyanin dye molecule to the conduction band of semiconductor TiO_2. The structure of the anthocyanin is shown in Scheme 1. R_1 and R_2 represent radicals, containing OH and OCH_3, characteristic from the *Anthocyanidin Petunidin* ($C_{16}H_{13}O_7^+$ (Cl^-)).

Further, in order to improve the conversion efficiency of DSSCs, another important key factor is concerning the film thickness of photoanode fabrication. Increasing the total interfacial surface area of the porous film by elevating the film thickness is easy, which enhances the amount of dye adsorbed and, thus, light absorption. Consequently, increasing the film thickness can increase the short-current density (J_{SC}) [17,18]. However, a film thickness also aggravates unnecessary charge recombination and poses more restrictions on mass transfer. Thus, both the open-current voltage (V_{OC}) and overall conversion efficiency are reduced [17–21]. Hence, the film thickness of the photoanode must be optimized to obtain efficient DSSCs. Numerous attempts have been done to improve the performance of DSSCs through the optimization of

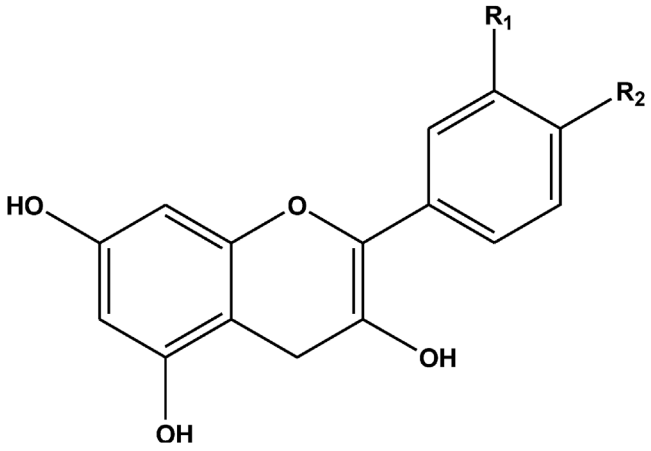

Scheme 1. Basic structure of anthocyanin molecule.

film thicknesses with different fabrication techniques of semiconductor photoanodes [22,23]. The dependence of TiO_2 photoanode film thickness on the enhanced performance of DSSC was optimized with 12.73 μm thickness by doctor-blade method [24]. Y-L. Lai et al. studied the influence of the TiO_2 film thicknesses with three different layers and optimized thickness was 7.67 μm. Further, increased the thickness of the film resulting decreased the photocurrent density and photovoltaic conversion efficiency, due to the lower light transmittance [25]. M. M. Byranvand et al. optimized the nano TiO_2 photoanode film thickness was 14 μm by tape casting technique [26]. I. Shin et al. analyzed the TiO_2 thickness effect on characteristics of a DSSC by electrochemical impedance spectroscopy (EIS) [27]. And also, several efforts have been made a compact, thin layer of semiconductor coated directly on the conducting glass substrate by spray pyrolysis [28,29], electrodeposition [30], screen-printing [27], dip-coating [31], doctor-blade [32,33] and spin-coating techniques [34].

In this work, the natural dye extracted from *Thunbergia erecta* natural flowers petals, which was optically characterized by ultraviolet–visible (UV–Vis), and Fourier transform infrared (FT-IR) spectroscopy. DSSC were fabricated using *Thunbergia erecta* extract with different thickness TiO_2 anodes. Morphological changes and depth profile were characterized by atomic force microscope (AFM) and field emission scanning electron microscope (FESEM). The photoelectrochemical properties (open circuit voltage (V_{OC}), short-circuit current density (J_{SC}), fill factor (*FF*), and conversion efficiency (η%) of the fabricated DSSCs using this extract as a photosensitizer were investigated.

2. Materials and methods

2.1. Materials

Conducting indium-doped tin oxide (ITO) coated glass substrates (10 Ω/cm^2) was received from Sigma Aldrich, USA. Analytical grade polyethylene glycol, nano TiO_2 (Degussa-P25) powder, potassium iodide and iodine salts were also obtained from Sigma Aldrich. All the other chemicals were analytical grade purchased and used from Sigma-Aldrich, without further purification.

2.2. Apparatus and instruments

The UV–Vis absorption spectra were recorded by Perkin Elmer (λ 650) spectrophotometer. The FTIR spectra were recorded by Agilent Cary 630 FTIR spectrometer. Surface topography, thickness and morphology of the photoanode thin films and cathode were measured by the use of atomic force microscopy (AFM) (Nanosurf EasyScan 2) and field emission scanning electron microscopy (FESEM) (JEOL®JSM-

7100F), respectively. The photovoltaic characteristics of the assembled DSSC devices were measured from an illuminated area of 0.5 cm × 0.5 cm by an IVIUM Compactstat multi-potentiostat with solar stimulator under standard AM 1.5 sunlight illumination with 100 mW/cm^2 light source. Electrochemical impedance spectroscopy (EIS) experiments were carried out in the range of 0.1–100 kHz within the alternating current amplitude of 10 mV at open circuit voltage (V_{oc}) under the condition of zero electric current.

2.3. Dye preparation

Natural flowers were collected from King's Mantle plant (*Thunbergia erecta*) in the Botanical garden in Rio de Janeiro, Brazil. The flowers were washed with isopropyl alcohol and subsequently dried at room temperature (in the case of *Thunbergia erecta*, only the petals were used). For the choice of solvents (acetone, ethanol, isopropyl alcohol or distilled water), tests were carried out respecting the same conditions to establish the most efficient dye extraction, which was the distilled water. After drying, the flowers were dipped in distilled water and mixed for a few minutes with the magnetic mixer. Finally, the solution was filtered and stored in an air-tight container for further applications in the freezer at 20 °C that can be kept for months.

2.4. Anode, cathode and electrolyte preparation

Initially, an Indium-doped SnO_2 conducting glasses (ITO) were cleaned with double distilled water, then acetone and isopropyl alcohol mixture (v/v = 1/1) in an ultrasound water bath for 20 min, and the electrodes were dried with a hot plate for proximally 10 min. The colloidal TiO_2 solution was prepared by adding 0.5 g of the P25 TiO_2 (Degussa-P25) nanopowder (~21 nm size), and 0.15 g of polyethylene glycol (PEG) in 3 mL of distilled H_2O and 3 mL of CH_3COOH (v/v = 1/1). The mixture was ultrasonicated for 2 h to form the homogeneous TiO_2 colloidal solution. The TiO_2 thin films (photoanode) were deposited over an ITO glass substrate with a layer-by-layer coating of the as-prepared TiO_2 colloidal solution using the spin-coating technique at 1000 rpm for 10 s. After that, the prepared electrodes were annealed at 450 °C for 30 min in an air atmosphere. The thickness of the TiO_2 photoanode is ~3.0 μm, ~5.5 μm, ~7.5 μm, ~12.0 μm and designates as 1-Layer, 2-Layer, 3-Layer and 4-Layer respectively.

The Pt counter-electrode was prepared by drop-casting of 2 mM hexachloroplatinic acid ethanolic solution on a conducting (ITO) glass and annealing at 350 °C for 30 min in air atmosphere.

During the experiments, the electrolyte was prepared an iodine-based redox electrolyte consisting of the mixture of a 0.8 g (0.5 M) solution of potassium iodide (KI) and 0.120 g (0.5 M) solution of iodine (I_2), 1:1 M ratio solubilized in 10 mL of acetonitrile to obtain the tri-iodide/iodide redox electrolyte.

2.5. Assembling and functioning of DSSC

To evaluate the performance of the *Thunbergia erecta* dye on TiO_2 thin film photoanodes, sandwich type cells were fabricated. Briefly, the various thicknesses of TiO_2 photoanodes were immersed in the *Thunbergia erecta* dye solution at ambient temperature for 24 h then washed to remove excess dye with isopropyl alcohol and dried subsequently. The Pt nanoparticle coated counter electrode was placed on top so that the conductive side of the counter electrode faced the dye-coated TiO_2 thin film and the cell was sealed on three sides with glue, one side was left open for the injection of an electrolyte solution. The cell electrolyte solution (0.5 M potassium iodide and 0.02 M iodine in acetonitrile) was injected through and was drawn into the space between the electrodes by capillary action.

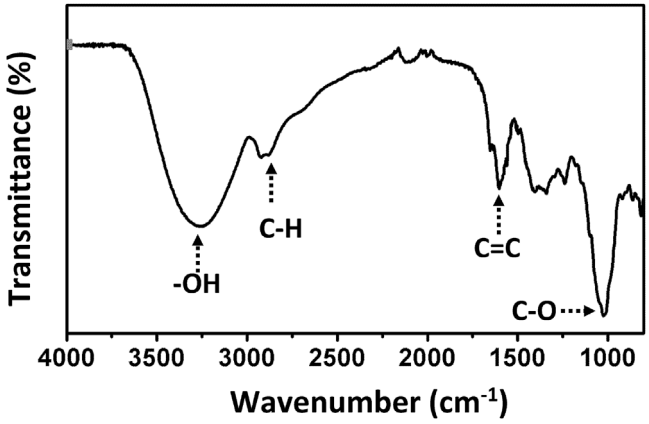

Fig. 2. FTIR spectra of extract obtained from petals of *Thunbergia erecta* flowers.

3. Results and discussion

3.1. Fourier transform infrared spectroscopy (FTIR)

Fig. 2 shows the FTIR spectrum of the dye extracted from *Thunbergia erecta* and shows most of the characteristic peaks of anthocyanin present in the dye sample [35]. The strong H—O—H band present in the region between 3000 and 3600 cm^{-1}, presence of water molecule in the dye samples, due to the water as used as a solvent and also the —OH stretching vibration of the anthocyanin part of dye is represented by a peak at 3260 cm^{-1}. As can be seen, the spectral region between 1600 and 1700 cm^{-1} confirms the infrared absorption of C═C and might be related to the vibration mode of the aromatic C═C in the anthocyanin molecule can be deduced by peak at 1608 cm^{-1} [36]. Consequently, the peak at 1665 cm^{-1} corresponds to the elongation vibration of the C═C double bond. The sharp stretching peak at 1016 cm^{-1} indicates the presence of the vibrational mode of stretching C—O—C. The spectrum also contains a stretching peak at 1716 cm^{-1} which were assigned to the C═O stretching vibration. This indicates that the anthocyanin dye molecule has a fractional quinonoidal form [37]. The two peaks at 2930 and 2873 cm^{-1} correspond to symmetric and asymmetric —CH stretching vibrations mode.

3.2. UV–visible absorption spectra

Absorption spectra offer the essential information on the absorption transition between the ground state and excited state of the dye molecule, and the solar energy range absorbed by the dye. Generally, anthocyanins and their derivates show a broad absorption band in the range of visible light attributed to charge transfer transitions from highest occupied molecular orbital (HOMO) to lowest unoccupied molecular orbital (LUMO) [38]. Anthocyanin contains from various plants, flowers, fruits and gave different photosensitizing performances [39]. Fig. 3 shows the light absorption ability of *Thunbergia erecta* flowers petals extract absorbed in the visible wavelength range of 400–800 nm with maxima at 537 nm, which is ascribed to the dye cores (anthocyanin) present in the flower's petal extracts and it can be considered as an efficient sensitizer for wide gap semiconductors [40]. Further, owing to the existence of hydroxyl and carbonyl groups present in the anthocyanin molecule can be easily bound the surface of the TiO_2 semiconducting film anodes, which was also confirmed in the FTIR analysis. These characteristics enhance the efficiency of the cell in the photovoltaic effect.

3.3. Surface characterization of photoelectrodes

Atomic force microscopy (AFM) was used to characterize the surfaces morphology of the multilayer photoanode samples. Topographic

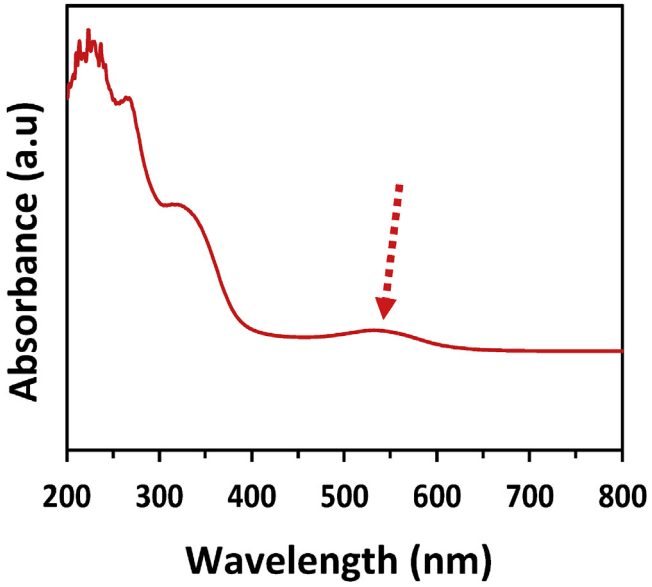

Fig. 3. UV–Vis absorption spectrum of the extract obtained from petals of *Thunbergia erecta* flowers.

images of the photoanode surfaces were taken in the conventional non-contact mode before dye loading onto TiO_2 film. Fig. 4 a-d shows the three dimension AFM images of the different TiO_2 thin film (thickness) annealed at 450 °C. The root mean square (RMS) roughness of the TiO_2 film was found to be 96 nm for 1-Layer, 99 nm for Layer-2, 74 nm for Layer-3, and 55 nm Layer-4 for the films annealed at 450 °C. TiO_2 particles are observed to be aggregated to form nanoclusters, which are useful for DSSC applications [18]. In fact, these nanoclusters form a porous structure which possesses not only a large surface area but also

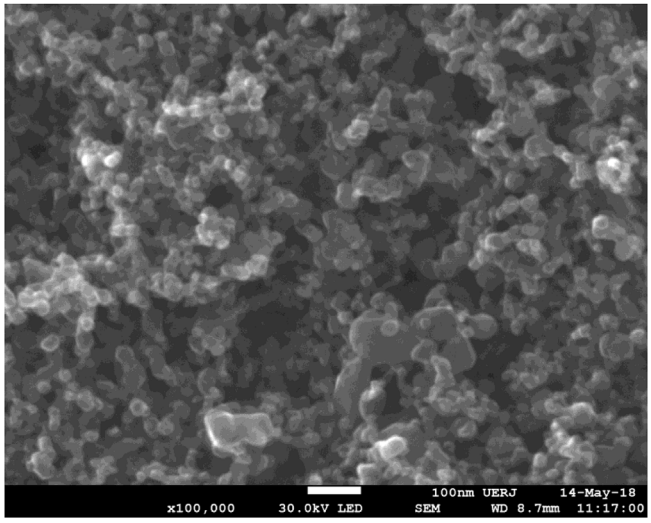

Fig. 5. Higher magnification FESEM image of the nanostructured TiO_2 photoanode.

facilitates more adsorption of dye molecules.

The surface morphology of the spin-coated TiO_2 thin film photoanodes under layer-by-layer was studied by field emission scanning electron microscopy (FESEM) analysis. The grain size, thickness, uniformity and porosity of the thin film were observed. Fig. 5 shows the FESEM images of nanostructured TiO_2, the grains sizes are around 20–25 nm and appear well connected each other with suitable mesoporosity to allow for a formation of an extended electrode-electrolyte interface. Moreover, observation indicates that the morphology of samples is very rough and may be beneficial to enhance the adsorption of dye due to its great surface roughness and high surface area. The FESEM images for the surface morphology and cross-sectional views of

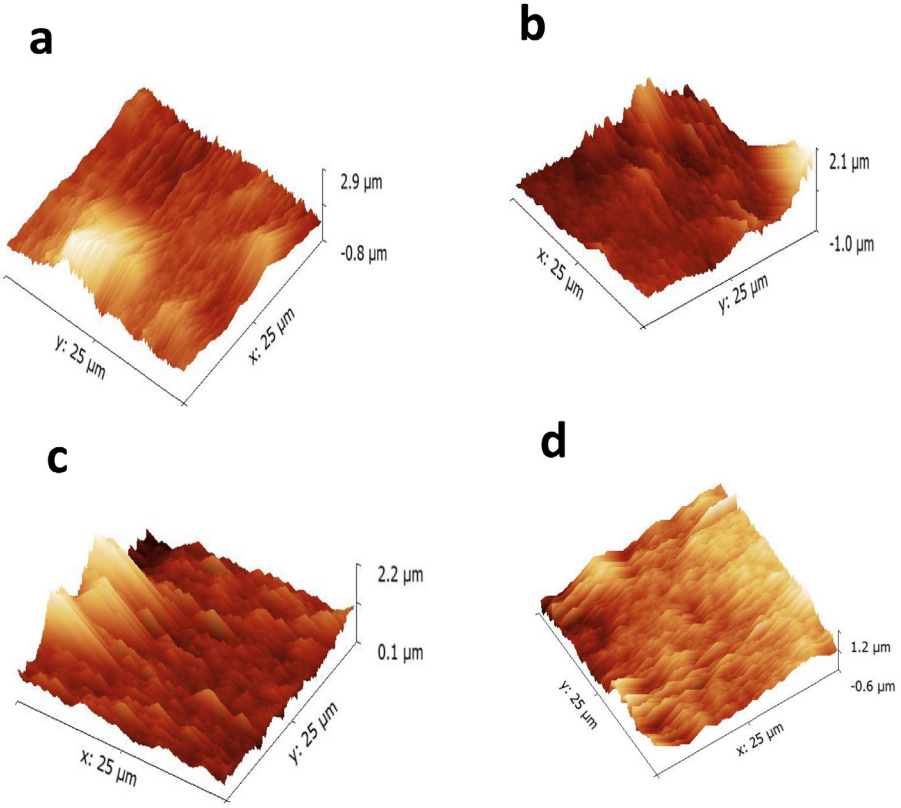

Fig. 4. Three-dimensional AFM images of (a) 1-Layer (b) 2-Layer (c) 3-Layer and (d) 4-Layer TiO_2 coated photoanodes.

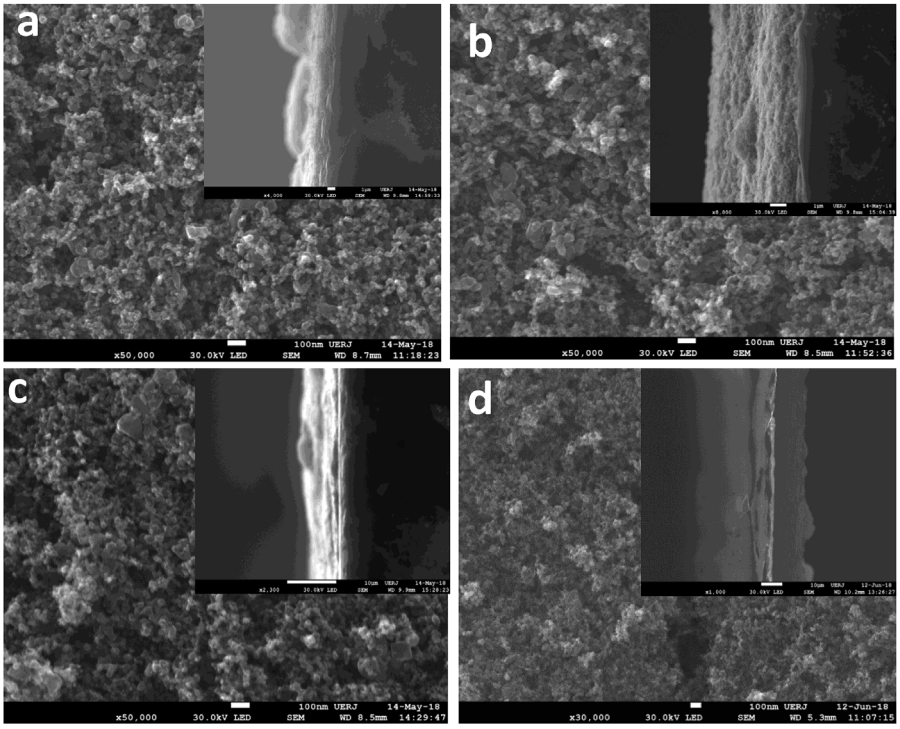

Fig. 6. FESEM images of (a) 1-Layer (b) 2-Layer (c) 3-Layer and (d) 4-Layer TiO_2-coated coated photoanodes. Insets: cross-sectional images for the estimation of TiO_2 film thickness.

the TiO_2 thin film photoanodes fabricated under different layers are shown in Fig. 6. The thickness values of the TiO_2 working electrodes fabricated under the layers 1, 2, 3 and 4 are ~3.0 μm, ~5.5 μm, ~7.5 μm and ~12.0 μm, respectively.

The surface morphology of the uncoated ITO glass substrates for comparison and Pt-coated photocathode were characterized by FESEM. The cathode showed hierarchical morphology after sintered at 350 °C is displayed in Fig. 7. These images indicate that Pt-coated homogenously in the electrode surface in nanostructured form. Such kind of hierarchical nanostructures enhances the electrocatalytic activity and conductivity of the electron transfer in the *J-V* performance in DSSC.

3.4. Photovoltaic performance

To compare the photocurrent density-voltage (*J-V*) characteristics of the fabricated DCCSs (1-Layer to 4-Layer TiO_2 electrodes) were measured under the illumination of 100 mWcm^{-2} (AM 1.5 G). The photovoltaic parameters of DSSCs with different TiO_2 thin film thickness are summarized in Table 1. Fig. 8a–d shows the dependence of various photovoltaic parameters on the TiO_2 film thickness: J_{SC}, V_{OC}, fill factor (FF), and overall conversion efficiency. As seen from Fig. 8c and Table 1, the short-circuit photocurrent density J_{sc} increases from 0.19 mA cm^{-2} to 0.27 mA cm^{-2} when the TiO_2 film thickness increases from 3.0 to 5.5 μm and then starts to decrease the photocurrent density when the film thickness increases above ~7.5 up to 12.0 μm. The open-circuit voltage (V_{OC}) decreases gradually as the thickness of TiO_2 photoanode increases. The result indicates that the recombination rate increases with the increase of layer by layer TiO_2 photoanode thickness. It is due to the elongated diffusion distance for the photoelectron to transport to the electrode enhancing the possibility of recombination. From *J–V* plot the values of short-circuit current (J_{sc}) and open-circuit

Table 1
Photoelectrochemical parameters for DSSC with multilayer TiO_2 thickness.

Photoanode	Thickness (μm)	J_{SC} (mA/cm^2)	V_{OC} (V)	FF	η (%)
Layer-1	3.0	0.19	0.56	0.34	0.22
Layer-2	5.5	0.27	0.55	0.40	0.37
Layer-3	7.5	0.25	0.54	0.32	0.26
Layer-4	12.0	0.15	0.50	0.42	0.19

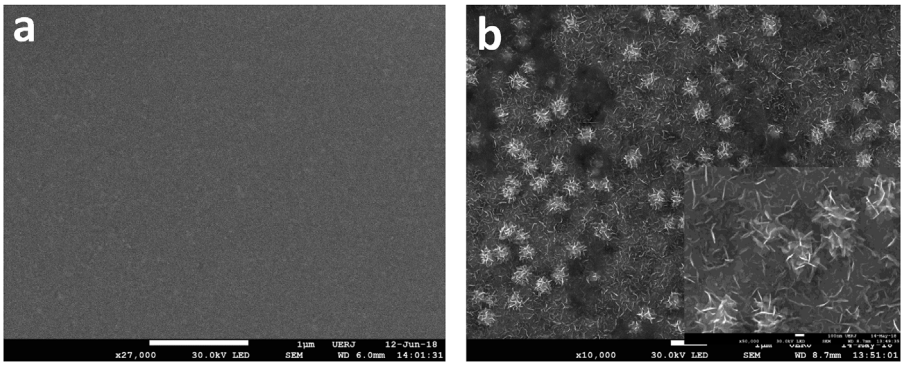

Fig. 7. FESEM images of (a) uncoated ITO and (b) Pt counter electrode.

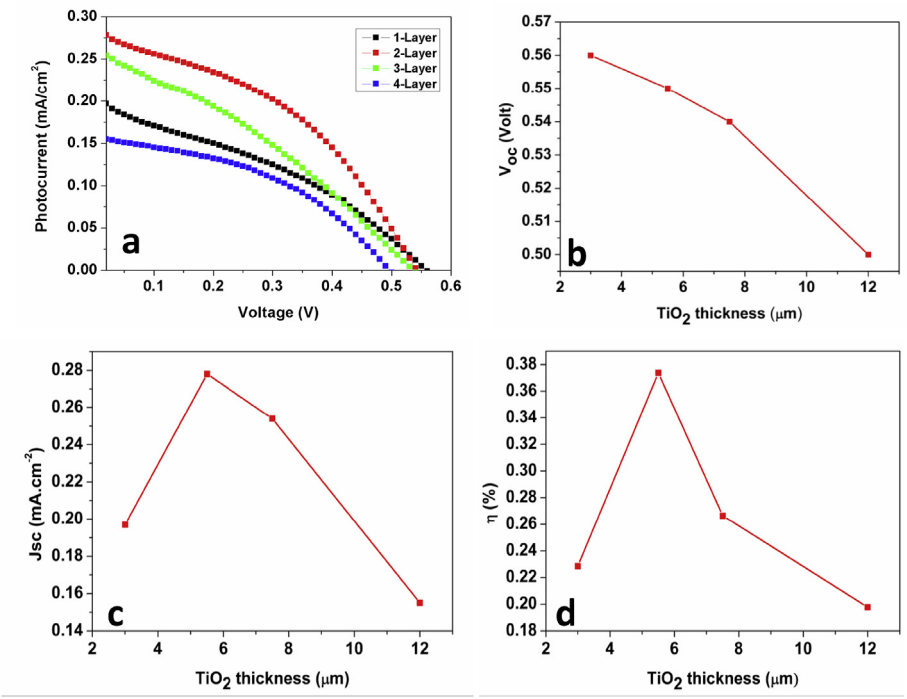

Fig. 8. (a) *J–V* curves (b, c and d) electrical characteristics (J_{sc}, V_{oc} and η) of the DSSCs using TiO_2 at different thicknesses as photoanodes.

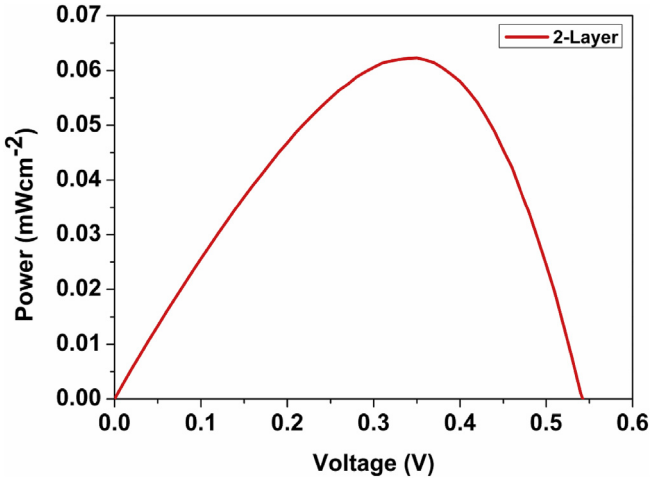

Fig. 9. Power versus voltage curve of the DSSC using the natural dyes extracted from the *Thunbergia erecta* flowers petals.

voltage (V_{oc}) of the DSSC were observed to be highest photocurrent density on 2-Layers (~5 μm) 0.27 mA/cm^2 and 560 mV respectively.

Commonly, the photocurrent density of DSSCs is governed by three major reasons: (a) the amount of photoexcited electrons, which is influenced by the capacity of dye molecules adsorption, (b) the rate of recombination at the interface of dye/TiO_2 thin film or TiO_2 thin film/electrolyte, and (c) the redox property of I^-/I_3^- in the electrolyte. Herein, the photoanode was coated with different thickness of the TiO_2 nanoparticles thin film. A precise thin layer photoanode induces a large surface area for improve dye molecules adsorption on the electrode surface. Therefore, an exact thickness of thin film photoanode captures extra light to produce more photoexcited electrons. However, the J_{SC} requires that these electrons successfully transport to the ITO electrode without recombination at the dye/photoanode or photoanode/electrolyte interfaces; therefore, electron diffusion length is also an important point that needs to be considered. Though a thin photoanode enhances the generation of photoexcited electrons, along electron diffusion length is unavoidable for those photoexcited electrons generated in the thick layer. Thus, the J_{SC} is an agreement between the two main factors: increased surface area by increasing photoanode thickness and increased thickness resulting in an extended electron diffusion path length. The experimental results signify that the optimized thickness is ~5.0 μm. Hence, 2-Layer photoelectrode has the highest photo-to-electron conversion efficiency of 0.37%.

The parameters of photovoltaic performance such as fill factor (FF) and overall conversion efficiency (η) of the cells were calculated using the following equations:

$$FF = J_{max} \times V_{max}/J_{sc} \times V_{oc} \quad (1)$$

$$\eta(\%) = J_{sc} \times V_{oc} \times FF/I_{Ins} \times 100 \quad (2)$$

Where J_{sc} is the short-circuit current density (mA cm^{-2}), V_{oc} the open-circuit voltage (V), and J_{max} (mA cm^{-2}) and V_{max} (V) are the current density and voltage respectively in the *J–V* curve, at the point of maximum power output. The values of fill factor and conversion efficiency obtained with different layers of TiO_2 thin film results were shown in Table 1. The maximum conversion efficiency obtained 0.37% for 2-Layers.

The maximum output power (P_{max}) is acquired by choosing a point on experimentally determined (*J–V*) curve corresponding to which the product of current (J_{max}) and potential (V_{max}) gives the maximum value. Fig. 9 shows the (power versus potential) curve for the DSSC and the corresponding power (P_{max}) obtained from *Thunbergia erecta* petal extracts was 62.3 μWcm^{-2}.

To further investigate the electric and electrochemical properties of the interfaces of the multi-layer TiO_2 photoanodes assembled with DSSCs based on the *Thunbergia erecta* petal extracts, EIS measurements were carried out [41]. In earlier reports, generally in DSSCs consists of two or three semicircles in the Nyquist plots [42,43]. The high frequency response is owing to the charge-transfer resistance at the Pt counter electrode/electrolyte interface, while in the mid-frequency regions corresponds to electron transport and transfer at TiO_2/dye/electrode interface. The low-frequency region reflects the Warburg diffusion process of I^-/I_3^- in the electrolyte [44]. The fitting results of EIS obtained are showed in Fig. 10(a–d) and the data analyzed and

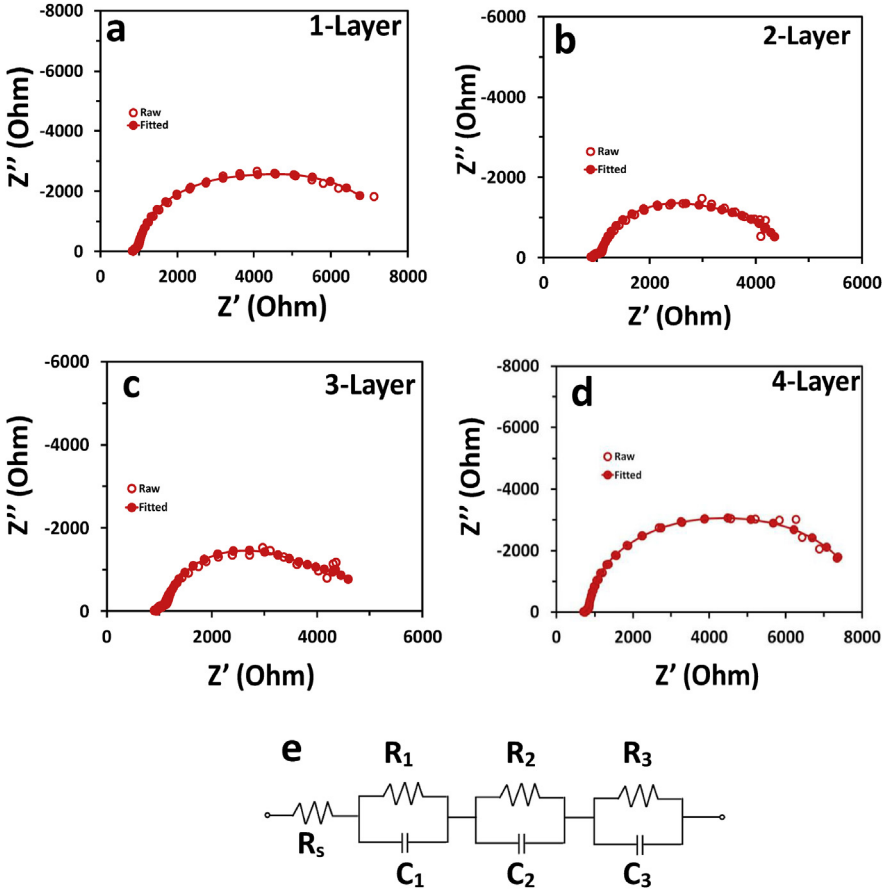

Fig. 10. EIS spectra of the DSSCs using (a) 1-Layer (b) 2-Layer (c) 3-Layer, (d) 4-Layer TiO_2-coated photoanodes and (e) corresponding equivalent circuit.

Table 2
Parameters obtained from EIS analysis for DSSCs with multilayer TiO_2 thickness photoanodes.

Electrodes	R_s(Ω)	R_1(Ω)	R_2(Ω)	R_3(Ω)	C_1(μF)	C_2(μF)	C_3(μF)
Layer-1	854.4	155.7	3060	3537	16.40	63.84	244.70
Layer-2	923.1	179.1	2223	1173	5.67	49.92	481.60
Layer-3	943.3	208.8	2599	1219	8.87	5.09	846.40
Layer-4	735.3	113.8	3630	3525	12.47	61.61	198.00

summarized in Table 2. The corresponding equivalent circuit (Fig. 10e) has been proposed and interprets the frequency of the assembled DSSCs. As shown in Fig. 10, the Nyquist plot contains two semicircles: the smaller semicircle in high frequency region is ascribed to the charge transfer resistance of the (R_{1ct}) values for the counter electrode (Pt/electrolyte) and the larger semicircle in mid-frequency range is related to the charge transport at dye adsorbed TiO_2/electrolyte interface resistance (R_2ct). The ohmic serial resistance (R_S) corresponds to the electrolyte and the ITO electrode and the (R_{3ct}) ascribed to Nernstian diffusion within the electrolyte. From Table 2, it is clear that the values of the charge transfer resistance (R_{2ct}) decreases with increasing TiO_2 film thickness from 3.0 to 5.5 μm but shows an increased charge transfer resistance with further increase in the film thickness from (5.5–12 μm). The results clearly revealed, the lowest charge transfer resistance values and highest J_{sc} and efficiency values correspond to DSSCs with optimum TiO_2 film thickness (5.5 μm, 2-Layer). The electron transfer between TiO_2/dye/electrolyte interfaces has been the most proficient and good, owing to the improved inter-particle connectivity and more conducting pathways of electrons coated by optimum thickness, surface area and porosity. Hence, optimizing the thin film thickness of nanostructured TiO_2 photoanodes are necessary in order to enhance the efficiency of DSSCs.

The DSSCs sensitized with extracts of lemon leaves (0.05%), turmeric (0.03%) [45], Ivy gourd fruits (0.09%) [46], Saraca ascoca flowers (0.09%) [47], Blue pea (0.05%), Annatto (0.19%), Norbixin (0.13%), Spinach (0.13%), Frutus lyciia (0.17%), Lily (0.17%) [48–51], and so on showed poor performances (less than 0.2%) compared to our dyes. Some of the dyes extracted from Begonia (0.24%), Ipomoea (0.27%), Marigold (0.23%), Tangerine peel (0.28%), China loropetal (0.27%), Chinese rose (0.27%), yellow rose (0.26%), Dragon fruit (0.22%) [50–52] and so on showed similar efficiencies to our dye.

4. Conclusions

In summary, the natural dye extract from the petals of *Thunbergia erecta* flowers were used as photosensitizers in TiO_2 multilayer film based DSSCs. Investigating the influence of the photoanode thickness were optimized the TiO_2 film (2-Layer 5 μm thick) for the best photoelectrochemical performances of DSSC device was studied. With such a fabricated DSSC, an open-circuit voltage (V_{oc}) of 0.55 V, short-circuit current density (J_{sc}) of 0.27 mA cm^2, P_{max} 62.3 μWcm^{-2}, fill factor (FF) of 0.40 and conversion efficiency of 0.37% could be obtained. The results indicate that increasing the thickness of thin film could enhance the surface area and increase the dye molecule adsorption, which improves the light absorbance as well as the generation of photoexcited electrons and long electron diffusion distance between the ITO electrode which increases the probability of recombination and results decrease the efficiencies. The conversion efficiency is expected to be further improved by introducing room temperature ionic liquids based I^-/I_3^- redox electrolytes in the future. Overall, natural *Thunbergia erecta* flowers dyes as sensitizers of DSSCs are promising because of their environmental friendliness, low-cost production, and renewable

modules. Hence, natural dyes as light harvesting constituents in DSSCs can contribute to a sustainable alternative for the future of energy production.

Acknowledgements

We are grateful to Dr. Victor Santos Ramos from Universidade do Estado do Rio de Janeiro (UERJ), Brazil and the students Mr. F. M. M. Santos, Mr. F. C. Ferreira from CEFET/RJ, Brazil for helping in the FESEM and AFM measurements. We also would like to thank the Brazilian funding agencies CAPES (BEX 5383/15-3), CNPq (301868/2017-4) and FAPERJ (E-26/110.087/2014,/213.577/2015 and /216.730/2015). Dr. R. Suresh Babu wishes to acknowledge CAPES for the financial assistance in the form of PNPD Scholarship and Mr. B.C. Ferreira would like to thank CNPq for the financial support.

References

[1] G. Richhariya, A. Kumar, P. Tekasakul, B. Gupta, Natural dyes for dye sensitized solar cell: a review, Renew. Sustain. Energy Rev. 69 (2017) 705–718.
[2] R. Neil, Optimizing dyes for dye-sensitized solar cells, Angew. Chem. Int. Ed. 45 (2006) 2338–2345.
[3] B. O'regan, M. Grätzel, A low-cost, high-efficiency solar cell based on dye-sensitized colloidal TiO_2 films, Nature 353 (1991) 737–740.
[4] M. Grätzel, Dye-sensitized solar cells, J. Photochem. Photobiol. C Photochem. Rev. 4 (2003) 145–153.
[5] S. Shalini, R. Balasundara Prabhu, S. Prasanna, T.K. Mallick, S. Senthilarasu, Review on natural dye sensitized solar cells: operation, materials and methods, Mater. Renew. Sustain. Energ. 4 (2015) 1306–1325.
[6] M.K. Nazeeruddin, A. Kay, I. Rodicio, R. Humphry-Baker, E. Mueller, P. Liska, N. Vlachopoulos, M. Grätzel, Conversion of light to electricity by cis-X_2Bis(2,2´-bipyridyl- 4,4´-dicarboxylate)ruthenium(II) charge-transfer sensitizers (X = Cl^-, Br^-, I^-, CN^-, and SCN^-) on nanocrystalline titanium dioxide electrodes, J. Am. Chem. Soc. 115 (1993) 6382–6390.
[7] S. Frederic, M.K. Fischer, A. Mishra, S.M. Zakeeruddin, M.K. Nazeeruddin, P. Bäuerle, M. Grätzel, A dendritic oligothiophene ruthenium sensitizer for stable dye-sensitized solar cells, Chem. Sus. Chem. 2 (2009) 761–768.
[8] M. Ryan, Progress in ruthenium complexes for dye sensitised solar cells, Platinum Met. Rev. 53 (2009) 216–218.
[9] N.A. Ludin, A.M. Al-Alwani Mahmoud, A.B. Mohamad, A.A.H. Kadhum, K. Sopian, N.S.A. Karim, Review on the development of natural dye photosensitizer for dye-sensitized solar cells, Renew. Sustain. Energy Rev. 31 (2014) 386–396.
[10] Y. Amao, T. Komori, Bio-photovoltaic conversion device using chlorine-e6 derived from chlorophyll from *Spirulina* adsorbed on a nanocrystalline TiO_2 film electrode, Biosens. Bioelectron. 19 (2004) 843–847.
[11] F.G. Gao, A.J. Bard, L.D. Kispert, Photocurrent generated on a carotenoid-sensitized TiO2 nanocrystalline mesoporous electrode, J. Photochem. Photobiol. Chem. 130 (2000) 49–56.
[12] K. Tennakone, A.R. Kumarasinghe, G.R.R.A. Kumara, K.G.U. Wijayantha, P.M. Sirimanne, Nanoporous TiO_2 photoanode sensitized with the flower pigment cyaniding, J. Photochem. Photobiol. Chem. 108 (1997) 193–195.
[13] Q. Dai, J. Rabani, Photosensitization of nanocrystalline TiO_2 films by anthocyanin dyes, J. Photochem. Photobiol. Chem. 148 (2002) 17–24.
[14] G. Calogero, G.D. Marco, Red Sicilian orange and purple eggplant fruits as natural sensitizers for dye-sensitized solar cells, Sol. Energy Mater. Sol. Cells 92 (2008) 1341–1346.
[15] I.C. Maurya, P. Srivastava, L. Bahadur, Dye-sensitized solar cells using extract from petals of male flowers *Luffa cyclindrica* L. as a natural sensitizer, Opt. Mater. 52 (2016) 150–156.
[16] H. Hug, M. Bader, P. Mair, T. Glatzel, Biophotovoltaics: natural pigments in dye-sensitized solar cells, Appl. Energy 115 (2014) 216–225.
[17] B. Tan, Y.Y. Wu, Dye-sensitized solar cells based on anatase TiO_2 nanoparticle/nanowire composites, J. Phys. Chem. B 110 (2006) 15932–15938.
[18] B. Lee, D.K. Hwang, P. Guo, S.T. Ho, D.B. Buchholtz, C.Y. Wang, R.P.H. Chang, Materials, interfaces, and photon confinement in dye-sensitized solar cells, J. Phys. Chem. B 114 (2010) 14582–14591.
[19] C.P. Hsu, K.M. Lee, J.T.W. Huang, C.Y. Lin, C.H. Lee, L.P. Wang, S.Y. Tsai, K.C. Ho, EIS analysis on low temperature fabrication of TiO2 porous films for dye sensitized solar cells, Electrochim. Acta 53 (2008) 7514–7522.
[20] Z.S. Wang, H. Kawauchi, T. Kashima, H. Arakawa, Significant influence of TiO_2 photoelectrode morphology on the energy conversion efficiency of N719 dye-sensitized solar cell, Coord. Chem. Rev. 248 (2004) 1381–1389.
[21] D.M. Sampaio, E. Thirumal, A.L.F. de Barros, The effect of photo-anode surface morphology and gel-polymer electrolyte on dye-sensitized solar cells with natural dyes, J. Mater. Sci. Mater. Electron. 27 (2016) 9953–9961.
[22] P.A. Connor, K.D. Dobson, A.J. McQuillan, New sol-gel attenuated total reflection infrared spectroscopic method for analysis of adsorption at metal oxides in aqueous solutions. Chelation of TiO_2, ZrO_2, and Al_2O_3 surfaces by catechol, 8-quinolinol, and acetylacetone, Langmuir 11 (1995) 4193–4195.
[23] N.J. Cherepy, G.P. Smestad, M. Grätzel, J.Z. Zhang, Ultrafast electron injection: Implications for a photoelectrochemical cell utilizing an anthocyanin dye-sensitized TiO_2 nanocrystalline electrode, J. Phys. Chem. B 101 (1997) 9342–9351.
[24] J.M.K.W. Kumari, N. Sanjeevadharshini, M.A.K.L. Dissanayake, G.K.R. Senadeera, C.A. Thotawatthage, The effect of TiO_2 photoanode film thickness on photovoltaic properties of dye-sensitized solar cells, Ceylon J. Sci. 45 (2016) 33–41.
[25] Y.-L. Lai, H.-R. Hsu, Y.-K. Lai, C.-Y. Zheng, Y.-H. Chou, N.-K. Hsu, G.-Y. Lung, Influence of thin film thickness of working electrodes on photovoltaic characteristics of dye-sensitized solar cells, MATEC Web of Conferences 123 (2017) 00030.
[26] M.M. Byranvand, A.N. Kharat, L. Fatholahi, Influence of nanostructured TiO_2 film thickness on photoelectrode structure and performance of flexible dye-sensitized solar cells, J. Nanostruct. 2 (2012) 327–332.
[27] I. Shin, H. Seo, M.-K. Son, J.-K. Kim, K. Prabakar, H.-J. Kim, Analysis of TiO_2 thickness effect on characteristic of a dye-sensitized solar cell by using electrochemical impedance spectroscopy, Curr. Appl. Phys. 10 (2010) S422–S424.
[28] J. Krüger, R. Plass, L. Cevey, M. Piccirelli, M. Grätzel, U. Bach, High efficiency solid-state photovoltaic device due to inhibition of interface charge recombination, Appl. Phys. Lett. 79 (2001) 2085.
[29] V. Baglio, M. Girolamo, V. Antonucci, A.S. Aricò, Influence of TiO_2 film thickness on the electrochemical behavior of dye-sensitized solar cells, Int. J. Electrochem. Sci. 6 (2011) 3375–3384.
[30] B.A. Gregg, F. Pichot, S. Ferrere, C.L. Fields, Interfacial recombination processes in dye-sensitized solar cells and methods to passivate the interfaces, J. Phys. Chem. B 105 (2001) 1422–1429.
[31] J.N. Hart, D. Menzies, Y.B. Cheng, G. Simon, L.C.R. Spiccia, TiO_2 sol-gel blocking layers for dye-sensitized solar cells, Chimie 9 (2006) 622–626.
[32] P. Schilinsky, C. Waldauf, C.J. Brabec, Performance analysis of printed bulk heterojunction solar cells, Adv. Funct. Mater. 16 (2006) 1669–1672.
[33] C.-Y. Huang, Y.-C. Hsu, J.-G. Chen, V. Suryanarayanan, K.-M. Lee, K.-C. Ho, The effects of hydrothermal temperature and thickness of TiO_2 film on the performance of a dye-sensitized solar cell, Sol. Energy Mater. Sol. Cells 90 (2006) 2391–2397.
[34] K. Norman, A. Ghanbari-Siahkali, N.B. Larsen, 6 Studies of spin-coated polymer films, Annu. Rep. Prog. Chem. 101 (2005) 174–201.
[35] K.V. Hemalatha, S.N. Karthick, C. Justin Raj, N.-Y. Hong, S.-K. Kim, H.-J. Kim, Performance of *Kerria japonica* and *Rosa chinensis* flower dyes as sensitizers for dye-sensitized solar cells, Spectrochim. Acta, Part A 96 (2012) 305–309.
[36] A.S. Polo, M.K. Itokazu, N.Y.M. Iha, Metal complex sensitizers in dye-sensitized solar cells, Coord. Chem. Rev. 248 (2004) 1343–1361.
[37] S. Hao, J. Wu, Y. Huang, J. Lin, Natural dyes as photosensitizers for dye-sensitized solar cell, Sol. Energy Mater. Sol. Cells 80 (2006) 209–214.
[38] P. Luo, H. Niu, G. Zheng, X. Bai, M. Zhang, W. Wang, Spectrochim. Acta, Part A 74 (2009) 936–942.
[39] K. Wongcharee, V. Meeyoo, S. Chavadej, Dye-sensitized solar cell using natural dyes extracted from rosella and blue pea flowers, Sol. Energy Mater. Sol. Cells 91 (2007) 566–571.
[40] S. Ananth, T. Arumanayagam, P. Vivek, P. Murugakoothan, Direct synthesis of natural dye mixed titanium dioxide nano particles by sol–gel method for dye sensitized solar cell applications, Optik 125 (2014) 495–498.
[41] Q. Wang, J. Moser, M. Grätzel, Electrochemical impedance spectroscopic analysis of dye-sensitized solar cells, J. Phys. Chem. B 109 (2005) 14945–14953.
[42] J. Van de Lagemaat, N.G. Park, A.J. Frank, Influence of electrical potential distribution, charge transport, and recombination on the photopotential and photocurrent conversion efficiency of dye-sensitized nanocrystalline TiO_2 solar cells: A study by electrical impedance and optical modulation techniques, J. Phys. Chem. B 104 (2000) 2044–2052.
[43] F. Fabregat-Santiago, J. Bisquert, E. Palomares, L. Otero, D. Kuang, S.M. Zakeeruddin, M. Grätzel, Correlation between photovoltaic performance and impedance spectroscopy of dye-sensitized solar cells based on ionic liquids, J. Phys. Chem. C 111 (2007) 6550–6560.
[44] K.-M. Lee, Y.-C. Hsu, M. Ikegami, T. Miyasaka, K.R.J. Thomas, J.T. Lin, K.-C. Ho, Co-sensitization promoted light harvesting for plastic dye-sensitized solar cells, J. Power Sources 196 (2011) 2416–2421.
[45] S. Suhaimi, M.M. Shahimin, Z.A. Alahmed, Y.J. Chysk, A.H. Reshak, Materials for enhanced dye-sensitized solar cell performance: electrochemical application, Int. J. Electrochem. Sci. 10 (2015) 2859–2871.
[46] V. Shanmugam, S. Manoharan, S. Anandan, R. Murugan, Performance of dye-sensitized solar cells fabricated with extracts from fruits of Ivy Gourd and flowers of Red Frangipani as sensitizers, Spectrochim. Acta, Part A 104 (2013) 35–40.
[47] I.C. Maurya, Neetu, A.K. Gupta, P. Srivastava, L. Bahadur, Natural dye extracted from Saraca asoca flowers as sensitizer for TiO_2-based dye-sensitized solar cell, J. Sol. Energy Eng. 138 (2016) 051006-1–051006-6.
[48] K. Wongcharee, V. Meeyoo, S. Chavadej, Dye-sensitized solar cell using natural dyes extracted from rosella and blue pea flowers, Sol. Energy Mater. Sol. Cells 91 (2007) 566–571.
[49] N.M. Gomez-Ortiz, I.A. Vazquez-Maldonado, A.R. Perez-Espadas, G.J. Mena-Rejon, J.A. Azamar-Barrios, G. Oskam, Dye-sensitized solar cells with natural dyes extracted from achiote seeds, Sol. Energy Mater. Sol. Cells 94 (2009) 40–44.
[50] H. Chang, H.M. Wu, T.L. Chen, K.D. Huang, C.S. Jwo, Y.J. Lo, Dye-sensitized solar cell using natural dyes extracted from spinach and ipomoea, J. Alloy. Comp. 495 (2010) 606–610.
[51] H. Zhou, L. Wu, Y. Gao, T. Ma, Dye-sensitized solar cells using 20 natural dyes as sensitizers, J. Photochem. Photobiol., A 219 (2011) 188–194.
[52] R.A.M. Ali, N. Nayan, Fabrication and analysis of dye-sensitized solar cell using natural dye extracted from dragon fruit, Int. J. Integr. Eng. 2 (2010) 55–62.